

## THE PRIMORDIAL LITHIUM ABUNDANCE

ROBERT L. KURUCZ

Harvard-Smithsonian Center for Astrophysics, 60 Garden Street, Cambridge, MA 02138

Received 1995 January 13; accepted 1995 March 21

### ABSTRACT

The D lines of Li I in extreme Population II stars hotter than 5500 K are highly temperature sensitive because lithium is nearly all ionized. A one-dimensional model atmosphere represents a space and time average over the actual three-dimensional, moving, hot and cold convective structure. Neutral Li does not have the average behavior represented by the one-dimensional model. Lithium is overionized by a factor of 10 so that the Li abundance computed from a one-dimensional model is too small by this same factor. Consequently,  $\log(N_{\text{Li}}/N_{\text{total}}) + 12 > 3.0$ .

This higher Li abundance resolves the only discrepancy in the radiatively driven cosmological model of the universe previously discussed by Kurucz. Because the baryon density is high enough to produce a flat, or nearly flat, universe, the number of stars can increase by a factor of 10, and the amount of radiation given off by those stars in the first billion years can increase by a factor of 10 over what is possible with a low baryon density. This model can explain the formation of Population III stars, globular clusters, galaxies, quasars, voids, galaxy clusters, streaming, and large-scale structure. It can explain isolated galactic evolution and morphology including bulges, disks, and abundances.

*Subject headings:* cosmology: theory — stars: abundances — stars: atmospheres — stars: Population II

### 1. INTRODUCTION

This is the third paper in a series on radiatively driven cosmology. The first two papers (Kurucz 1992, 1993a) demonstrate that a big bang universe consisting, before recombination, of a statistically uniform gas of H, D,  $^3\text{He}$ ,  $^4\text{He}$ , and Li ions, electrons, photons, and massless neutrinos at a density sufficient, or nearly sufficient, to produce a flat universe, can evolve into the universe as we now observe it, with large-scale structure and a smooth microwave background. Evolution during the first billion years is controlled by radiation. If the baryon density is 10 times what cosmologists now assume, there can be 10 times as many stars, and 10 times as much radiation from stars. This model explains the formation of Population III stars, globular clusters, galaxies, quasars, voids, galaxy clusters, streaming, and large-scale structure. It explains isolated galactic evolution and morphology including bulges, disks, and abundances. There is one crucial observation that the model does not explain. It predicts a primordial Li abundance 10 times higher than the value commonly assumed by cosmologists (e.g., Boesgaard & Steigman 1985; Kolb & Turner 1990). It also predicts that primordial deuterium is reduced by a factor of 100 and that primordial  $^3\text{He}$  is reduced by a factor of 10. In extreme Population II stars with effective temperatures between 5500 and 6500 K, abundance analyses (Spite & Spite 1982; Rebolo, Molaro, & Beckman 1988) yield approximately constant  $\log(N_{\text{Li}}/N_{\text{total}}) + 12 = 2.1$ . The measured abundance is the primordial abundance plus a small addition from spallation of CNO by the supernovae that poisoned the star-forming gas with metals. The spallation fraction can be estimated from Be and B created in the same way. There are small losses from burning and from diffusion. The observed abundance is expected to be the lower limit for the primordial abundance. For radiatively driven cosmology,  $\log(N_{\text{Li}}/N_{\text{total}}) + 12 > 3.0$ . My initial solution to this problem was to argue that the extreme Population II stars did not have the primordial Li abundance. I assumed that the state of the art for

modeling interiors is as poor as that for modeling atmospheres so that 90% could have been removed by diffusion (Michaud, Fontaine, & Beaudet 1984) or by increased convective burning at the beginning of the star's life (D'Antona & Mazzitelli 1984). But now I have been convinced by the constancy of the Li abundance determinations over a range of metal abundances and temperatures that the Li is primordial or nearly primordial.

What are the other possibilities? Thirty years ago, the derived Fe abundance in the Sun was smaller by a factor of 10 than the present value because of bad *gf*-values (Goldberg, Müller, & Aller 1960; Goldberg, Kopp, & Dupree 1964). It took decades to solve, or nearly to solve, this problem. But the *gf*-values for the Li D lines are relatively easy to compute; they cannot be off by a large percentage. The only possibility remaining, if the Li abundance is high, is that the model atmospheres used in the abundance analysis are wrong. In this paper I explain how the conventional analysis is in error and present a qualitative model of convection that shows that Li is strongly overionized in extreme Population II stars relative to Li in existing models, even in convective layers, so that the abundance is much higher than is determined from simple models.

We assume that the deuterium in these extreme Population II stars is also primordial. Lubowich et al. (1994) were unable to detect deuterium ( $\text{D}/\text{H} < 10^{-5}$ ) in HD 140283, one of the brightest of these stars.

### 2. WHEN IS PHYSICS VALID?

Every observation, measurement, model, and theory has seven characteristic numbers: resolution in three space coordinates, in time, and in energy, minimum energy, and maximum energy. Many people never think about these resolutions. A low-resolution physics cannot be used to study something in which the physical process of interest occurs at high resolution unless the high-resolution effects average out when integrated

over the resolution bandpasses. If a theory is statistical, it cannot be valid if the resolution volume does not contain a large number of particles.

In order to understand the Li abundances, we must consider the theory and observation of stellar atmospheres. What does the Sun, or any convective atmosphere, actually look like? We do not really know yet. There is a very simplified three-dimensional radiation-hydrodynamics calculation discussed in the review by Chan et al. (1991, pp. 223–274). It is consistent with the high spatial and temporal resolution observations shown in the review by Topka & Title (1991, pp. 727–747). We can qualitatively understand the problem by studying Figure 1 taken from Chan et al. This is a plot of the fluid velocity in an  $x$ - $z$  plane cut through their three-dimensional box. To quote them exactly: “The ascending flow is broad and diverging; the descending flow is filamentary and converging. The cells span the entire vertical extent of the computational domain. There are no multiple cells in the vertical direction.” The rising elements are hot, and the falling elements are cold. The filling factor for the cold downward flowing elements is small. The structure changes with time. Nordlund & Dravins (1990) discuss four similar stellar models with many figures.

There is a solar flux atlas (Kurucz et al. 1984) that Ingemar Furenlid caused to be produced because he wanted to work with the Sun as a star for comparison to other stars. The atlas is pieced together from eight Fourier transform spectrograph scans, each of which was integrated for 2 hr, so the time resolution is 2 hr for a given scan. But the scans were made over an 8 month period. For studying variability, the resolution can be as bad as 8 months. The  $x$  and  $y$  resolutions are the diameter of the Sun. The  $z$  resolution (from the formation depths of features in the spectrum) is difficult to estimate. It depends on the signal-to-noise ratio and the number of resolution elements. The first is greater than 3000, and the second is more than  $10^6$ . It may be possible to find enough weak lines in the wings and shoulders of strong lines to map out relative positions to a few kilometers. Currently, the  $z$  resolution is typically a few tens of kilometers. The resolving power is on the order of 522,000. This is not really good enough for observations made through the atmosphere because it does not resolve the terrestrial lines that must be removed from the spectrum. The Sun itself degrades its own spectrum by differential rotation and macroturbulent motions. The energy range is from 300 to 1300 nm, essentially the range where the Sun radiates most of its energy.

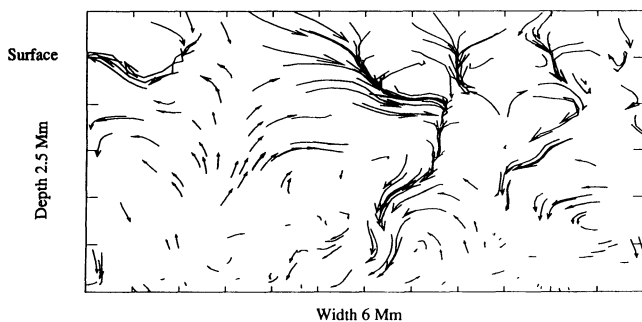


FIG. 1.—Simplified three-dimensional radiation-hydrodynamics calculation discussed in the review by Chan et al. (1991), figure used with permission of authors. The plot is of fluid velocity in an  $x$ - $z$  plane cut through their three-dimensional box. The rising elements are hot, and the falling elements are cold. The filling factor for the cold downward flowing elements is small. The structure changes with time.

To analyze this spectrum, or any other spectrum, we need a theory that works at a similar resolution or better. We use a plane-parallel, one-dimensional theoretical or empirical model atmosphere that extends in  $z$  through the region where the lines and continuum are formed. The one-dimensional model atmosphere represents the space average of the convective structure over the whole diameter of the star (including the center-to-limb variation) and the time average over hours. It is usually possible to compute a model that matches the observed energy distribution around the flux maximum. However, to obtain the match it is necessary to adjust a number of free parameters: effective temperature, surface gravity, microturbulent velocity, and the mixing length-to-scale height ratio in the one-dimensional convective treatment. The microturbulent velocity parameter also produces an adjustment to the line opacity to make up for missing lines. Since much of the spectrum is produced near the flux maximum, at depths in the atmosphere where the overall flux is produced, averaging should give good results. The parameters of the fitted model may not be those of the star, but the radiation field should be like that of the star. The Sun is the only star where the effective temperature and gravity are accurately known. In computing the detailed spectrum, it is possible to adjust the line parameters to match all but the centers of the strongest lines. Since very few lines have atomic data known accurately enough to constrain the model, a match does not necessarily mean that the model is correct.

### 3. FINDING ERRORS

There is ample precedent for order of magnitude errors in abundances. The early determinations of the solar Fe abundance were too small by a factor of 10 because of poor  $gf$ -values; see Goldberg et al. (1960, 1964). Between the first and second of these papers, Corliss & Bozman (1962) measured  $gf$ -values for 25,000 lines, including 658 for Fe I. Corliss & Warner (1964) redid the Fe I  $gf$ -values and measured 2000 lines. Goldberg et al. (1964) used those measurements to find the iron abundance. It came out nearly the same. It is only in the present decade that the error has been reduced below 50%. But it may not be as low as the 10% claimed in modern papers.

One should always question atomic data, observational data, and model atmospheres, including one's own. There can be errors in the programs that are not discovered until some extreme case is considered. The users of such data and models must always consider the possibility of error.

### 4. THE ERROR

There are two fundamental rules of abundance analysis: (1) use weak lines on the linear part of the curve of growth where line strength is directly proportional to abundance, and (2) work with the principal stage of ionization. These rules minimize the effects of errors in the model, in the damping treatment, and in microturbulent velocity. If there is a factor of 2 error in the ionization of a 90% ionized element, the neutral abundance is in error by a factor of 2 while the ion abundance is in error only by 5%.

P. Molaro pointed out to me that the Li abundance is sensitive to the convective treatment in my models. Molaro, Bonifacio, & Primas (1995) have computed models with various convective treatments to try to estimate the uncertainty. My initial view of these results was to believe that the mixing-length theory was seriously deficient (giving an error of 50%–500% in the Li abundance) and that no one is capable of computing real convection. After further discussion with

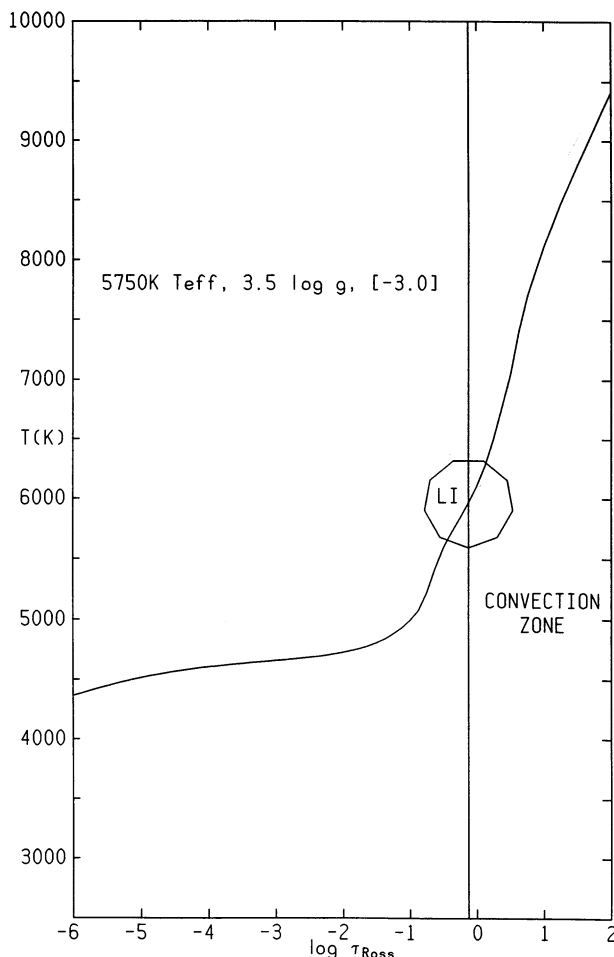


FIG. 2.—A model from the Kurucz (1993b) grid that has the approximate parameters for HD 140283:  $T_{\text{eff}} = 5750$  K,  $\log g = 3.5$ , and  $\log$  metal abundance of  $[-3.0]$  relative to solar. The Schwarzschild-criterion top of the convection-zone and the depth of formation of the D lines are indicated.

Molaro at the 1994 IAU General Assembly in the Hague, it occurred to me that if the Li D lines are so sensitive, they must be formed at the top of the convection zone. I examined a model from the Kurucz (1993b) grid that has the approximate parameters for HD 140283, one of the brightest extreme Population II stars: 5750 K  $T_{\text{eff}}$ , 3.5  $\log g$ , and  $[-3.0]$ . The model is more strongly convective than a solar model; the convective velocity is  $3.0 \text{ km s}^{-1}$  instead of 2.2 in the solar model. The higher convective velocity implies higher microturbulent and macroturbulent velocities as well. The model is plotted in Figure 2 with the Schwarzschild-criterion top of the convection zone and the depth of formation of the D lines marked. Li is more than 99.94% ionized at that depth. The chance that the Li abundance can be found by using a one-dimensional model atmosphere is therefore essentially zero. It can be determined only by doing a real three-dimensional radiation-hydrodynamics convection calculation that is computationally between 100 and 1000 times the current state of the art because of the complexity of treating the radiative transfer realistically.

## 5. LITHIUM

The Li abundance determination has been assumed to be a straightforward problem, and the Population II observers were thought to be treating it correctly. I have computed the Li D line region in the Sun as part of computing the whole spectrum to test my line data as shown in Figure 3. Few people realize that in the Sun one-half the lines are still not identified. In Figure 3 there are large numbers of lines in the spectrum stronger than the Li lines that are completely missing from the line list. The 19 components of the D lines are listed in Table 1. The other lines that are deeper than 0.001 in residual flux are listed in Table 2. Most of the lines are from the CN molecule. In extreme Population II stars where the Li abundance is higher than in the Sun and the metal abundance is much lower, the missing lines do not matter. They may matter in Population I stars.

TABLE 1

ISOTOPIC AND HYPERFINE COMPONENTS OF THE Li D LINES

WL (air) (nm)	$\log gf$	$J_{lo}$	$E_{lo}$	$J_{up}$	$E_{up}$	Hyperfine	Isotope
670.7749.....	0.002	0.5	-0.034	1.5	14903.983	-1.204 1-0	7, -0.034
670.7749.....	0.002	0.5	-0.034	1.5	14903.983	-0.806 1-1	7, -0.034
670.7749.....	0.002	0.5	-0.034	1.5	14903.983	-0.806 1-2	7, -0.034
670.7773.....	0.002	0.5	0.020	1.5	14903.983	-1.505 2-1	7, -0.034
670.7773.....	0.002	0.5	0.020	1.5	14903.983	-0.806 2-2	7, -0.034
670.7773.....	0.002	0.5	0.020	1.5	14903.983	-0.359 2-3	7, -0.034
670.7899.....	-0.299	0.5	-0.034	0.5	14903.649	-0.505 1-2	7, -0.034
670.7900.....	-0.299	0.5	-0.034	0.5	14903.646	-1.204 1-1	7, -0.034
670.7918.....	0.002	0.5	-0.008	1.5	14903.632	-0.829 0-0	6, -1.125
670.7918.....	0.002	0.5	-0.008	1.5	14903.632	-0.732 0-1	6, -1.125
670.7923.....	-0.299	0.5	0.020	0.5	14903.649	-0.505 2-2	7, -0.034
670.7924.....	0.002	0.5	0.004	1.5	14903.632	-1.732 1-0	6, -1.125
670.7924.....	0.002	0.5	0.004	1.5	14903.632	-0.829 1-1	6, -1.125
670.7924.....	0.002	0.5	0.004	1.5	14903.632	-0.301 1-2	6, -1.125
670.7925.....	-0.299	0.5	0.020	0.5	14903.646	-0.505 2-1	7, -0.034
670.8069.....	-0.299	0.5	-0.008	0.5	14903.297	-0.528 0-1	6, -1.125
670.8070.....	-0.299	0.5	-0.008	0.5	14903.296	-1.431 0-0	6, -1.125
670.8074.....	-0.299	0.5	0.004	0.5	14903.297	-0.431 1-1	6, -1.125
670.8075.....	-0.299	0.5	0.004	0.5	14903.296	-0.528 1-0	6, -1.125

NOTES.—The subscripts “lo” and “up” refer to lower and upper energy levels. “WL(air)” stands for air wavelength in nm,  $E$  is the energy level in wavenumbers, “Hyperfine” refers to log fractional strength of the hyperfine component between  $F_{lo}$  and  $F_{up}$ , and finally the isotope column lists the isotope and the log isotopic abundance.

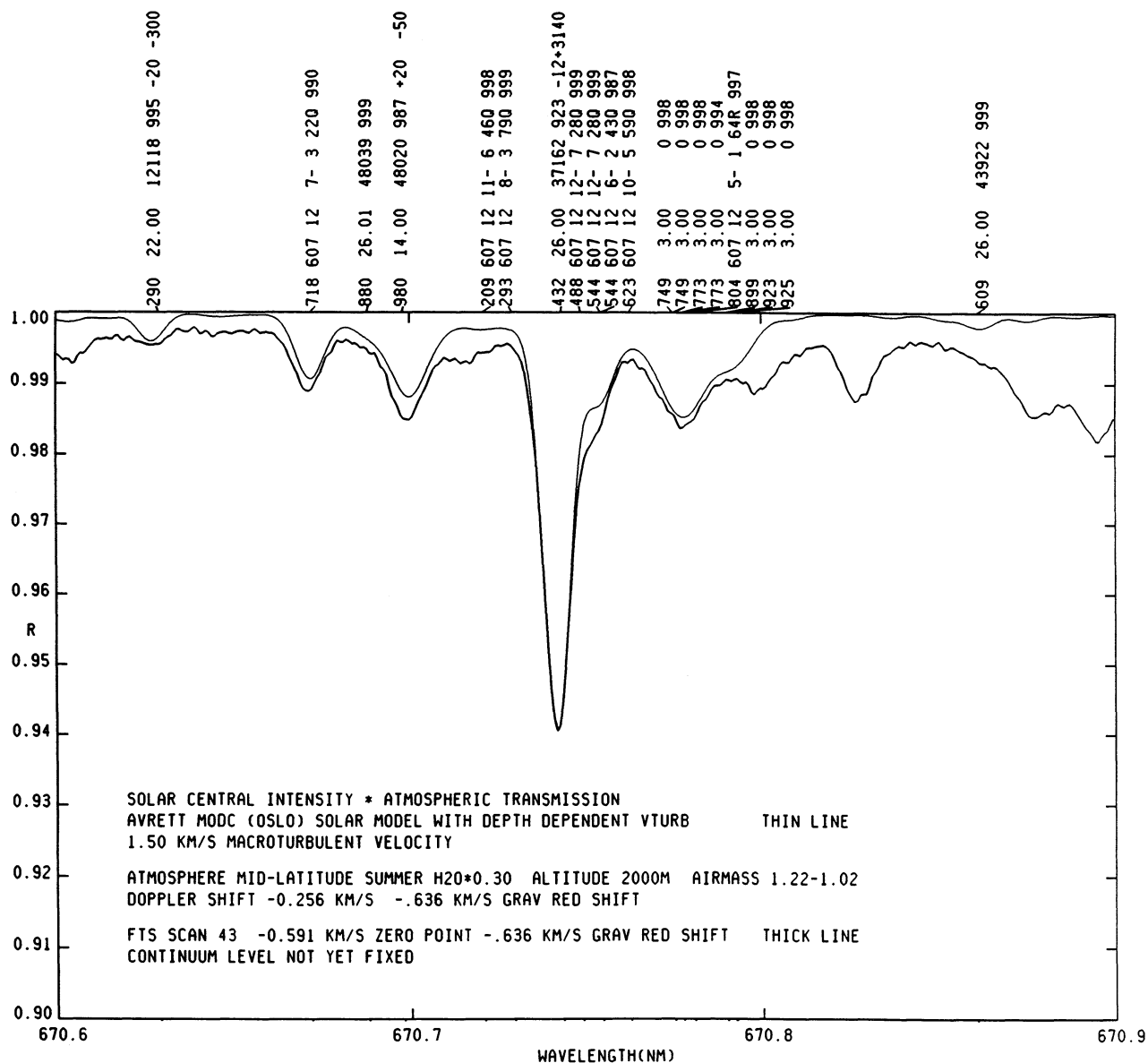


FIG. 3.—The computed Li D line region in the Sun. Detailed identifications are given in Tables 1 and 2. The first number in each label is the last three digits of the wavelength. The last number is the residual intensity (continuum = 1000) at line center if the line were computed in isolation. The signed numbers are wavelength or  $\log gf$  adjustments described in Table 2.

The mixing-length theory itself produces a temperature bifurcation that is assumed to average out in the physics. I use an old model atmosphere program, ATLAS11, to demonstrate this bifurcation. It uses a two-stream mixing-length formulation in which half the area of the star is a hot upward stream and the other half is a cold downward stream. Figure 4 shows the temperature bifurcation that program produces from the mean model. There can be 3000 K temperature differences, but they are constrained to the convection zone.

The more realistic three-dimensional calculations show that hot and cold streams continue toward the surface and also that the hot streams are 80% or 90% of the area. It seemed to be better to consider self-consistent single-component models with a range of effective temperatures. In Figure 5 the mean 5750, 3.5, [-3] model and its siblings within 1000 K are

plotted. It shows a temperature range qualitatively similar to that shown for a three-dimensional model in Figure 19c in Nordlund & Dravins (1990). Also plotted for each model is the log fraction of neutral lithium over total lithium. The neutral fraction is determined mainly by the electron number density which increases by 6 orders of magnitude from top to bottom of the atmosphere.

For each of the nine models a complete non-LTE calculation for Li was done, including all levels and lines up through  $n = 9$ . The equivalent width of the D lines was computed, assuming no  $^6\text{Li}$ , both for Li abundance 2.08 and 3 as listed in Table 3. The non-LTE effect was never more than a few percent in accordance with Carlsson et al. (1994). In retrospect, the whole calculation could have been done in LTE with the same results. The mean model has approximately the observed

TABLE 2  
LINES DEEPER THAN 0.001 IN RESIDUAL FLUX

Line	WL (air) (nm)	log $gf$	$J_{lo}$	$E_{lo}$	$J_{up}$	$E_{up}$	Code <sup>a</sup>	Label (lo) <sup>b</sup>	label (up) <sup>b</sup>
Si I .....	670.6980	-2.480	1.0	48020.074	1.0	62925.800	14.00	p4p 3D	p6d 3D
Ti I .....	670.6290	-2.508	4.0	12118.394	4.0	27025.652	22.00	s2 a1G	(1D)sp x3F
Fe I .....	670.7432	-5.531	2.0	52067.460	2.0	37162.740	26.00	s6D)4d e5P	a4F)4p y3F
	670.8609	-3.405	2.0	58824.770	3.0	43922.664	26.00	s4D)4d g5G	(3P)sp w5D
Fe II .....	670.6880	-4.100	2.5	48039.090	3.5	62945.038	26.01	d7 d2D1	(3F)4p x4D
CN .....	670.6718	-1.771	22.5	6977.132	22.5	-21883.509	607.00	X03 1	A07f1 12
	670.7209	-1.443	46.5	-15854.368	46.5	-30760.219	607.00	X06 2	A11e2 12
	670.7293	-1.432	79.5	-17692.027	79.5	-32598.258	607.00	X03 2	A08e2 12
	670.7488	-1.709	28.5	-15276.300	28.5	-30181.216	607.00	X07 2	A12e2 12
	670.7544	-1.709	28.5	-15174.589	28.5	-30079.474	607.00	X07 1	A12f1 12
	670.7544	-1.594	43.5	7708.482	43.5	-22612.592	607.00	X02 2	A06e2 12
	670.7623	-1.348	59.5	-16461.994	59.5	-31367.003	607.00	X05 2	A10e2 12
	670.7804	-1.967	64.5	9726.480	65.5	-24630.114	607.00	X01 1	A05e1 12

NOTES.—CN wavelengths are laboratory values from J. Brault. The Fe I  $\lambda$ 670.7432 line is from the multiplet table by Nave et al. 1994 and a new calculation by Kurucz. All other numbers are from Kurucz 1993c. Negative energies are predicted. The Si I line was adjusted by +0.0020 in WL and -0.050 in log  $gf$ . The Ti I line was adjusted by -0.0020 and -0.300. The Fe I  $\lambda$ 670.7432 line was adjusted by -0.0012 and +3.140 in agreement with the laboratory intensity.

<sup>a</sup> Identification for the species in the Kurucz 1993c line lists.

<sup>b</sup> Spectroscopic identifier for the state.

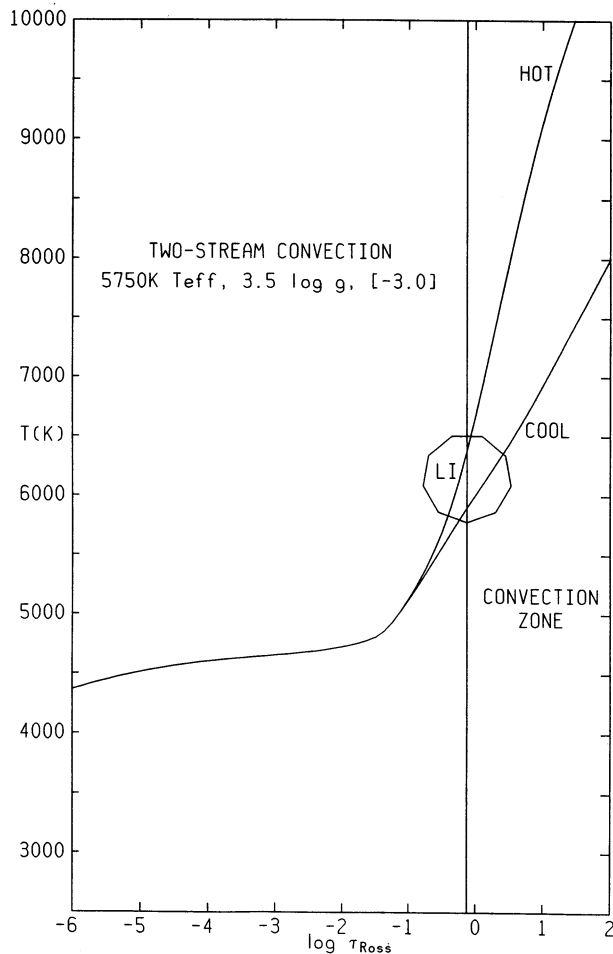


FIG. 4.—The temperature bifurcation produced by the ATLAS11 program for the mean model shown in Fig. 2. ATLAS11 uses a two-stream mixing-length formulation in which half the area of the star is a hot upward stream and the other half is a cold downward stream.

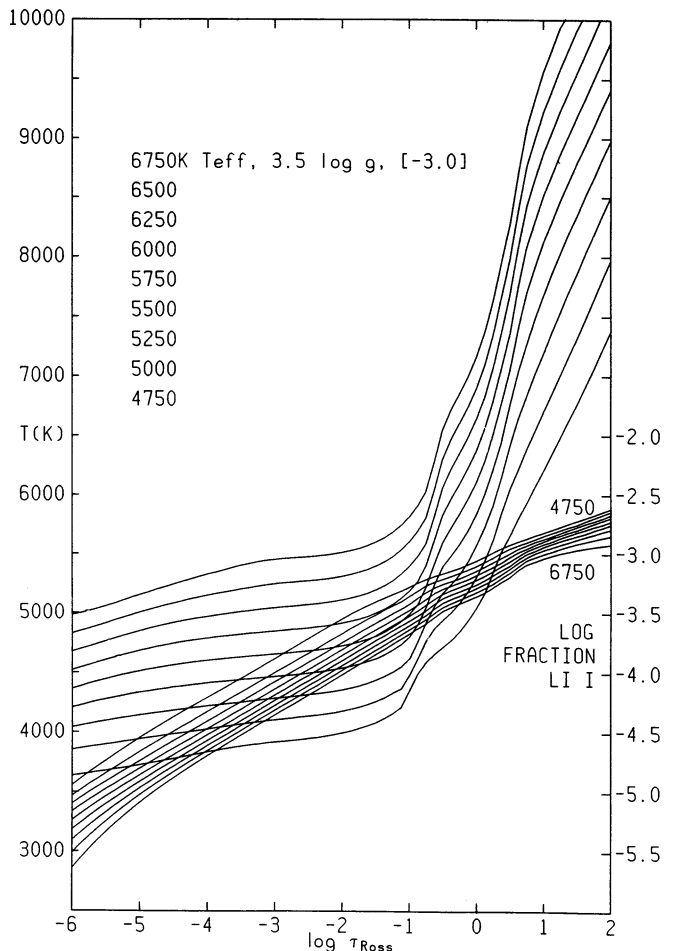


FIG. 5.—The mean model and its siblings within 1000 K from the Kurucz (1993b) grid. The log fraction of neutral Li is also plotted.

TABLE 3  
NON-LTE Li D EQUIVALENT WIDTHS (in mÅ)

$T_{\text{eff}}$ (K)	log Li ABUNDANCE	
	2.08	3.0
4750 .....	166	276
5000 .....	122	238
5250 .....	88	208
5500 .....	62	180
5750 .....	43	150
6000 .....	29	121
6250 .....	20	94
6500 .....	14	71
6750 .....	9	52

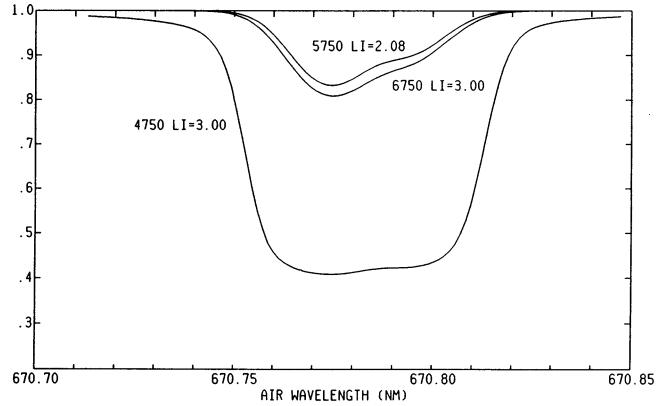


FIG. 6.—Non-LTE Li D residual flux profiles computed for the hot, cold, and mean models. The mean model with a standard Li abundance has approximately the observed equivalent width for HD 140283, as does the model which is 1000 K hotter with high Li abundance. The cold model has a 6 times larger equivalent width for the high abundance, and it also has a wide rectangular profile.

equivalent width for HD 140283. So does the model which is 1000 K hotter with high abundance. The cold model has a 6 times larger equivalent width for the high abundance and it also has a wide rectangular profile. The profiles are plotted in Figure 6. A two-component model with 80%–90% of the surface hot and the remainder cold would produce the wrong equivalent width. It would also produce a bimodal line with a shallow rectangular base and a triangular center, unlike the purely triangular profile actually observed (Hobbs & Thorburn 1994). The observed profile is similar to the triangular profiles in Figure 6 and shows that less than roughly 3%, and perhaps none of the observed space-time volume, has strong Li D lines. Figure 7 shows the mean intensity in the Balmer continuum for the hot and cold models at the depth of formation of the D lines in the mean model. The  $^2S$  continuum starts at 230 nm. The  $^2P$  continuum starts at 350 nm. The mean intensity is between 1–2 orders of magnitude greater in the hot

component. Figure 7 also shows the total opacity at the same point. The cold component is 15 times more transparent because it has a much lower  $H(n=2)$  population. The cold components cannot be optically thick to the ionizing radiation from the hot component. Therefore, Li is overionized in the cold component. In a real convective calculation, the cool component is filamentary and the transfer is computed in all directions. The final result will be that the real star with 10 times as much Li produces the same equivalent width as that produced by a one-dimensional model with 2.08.

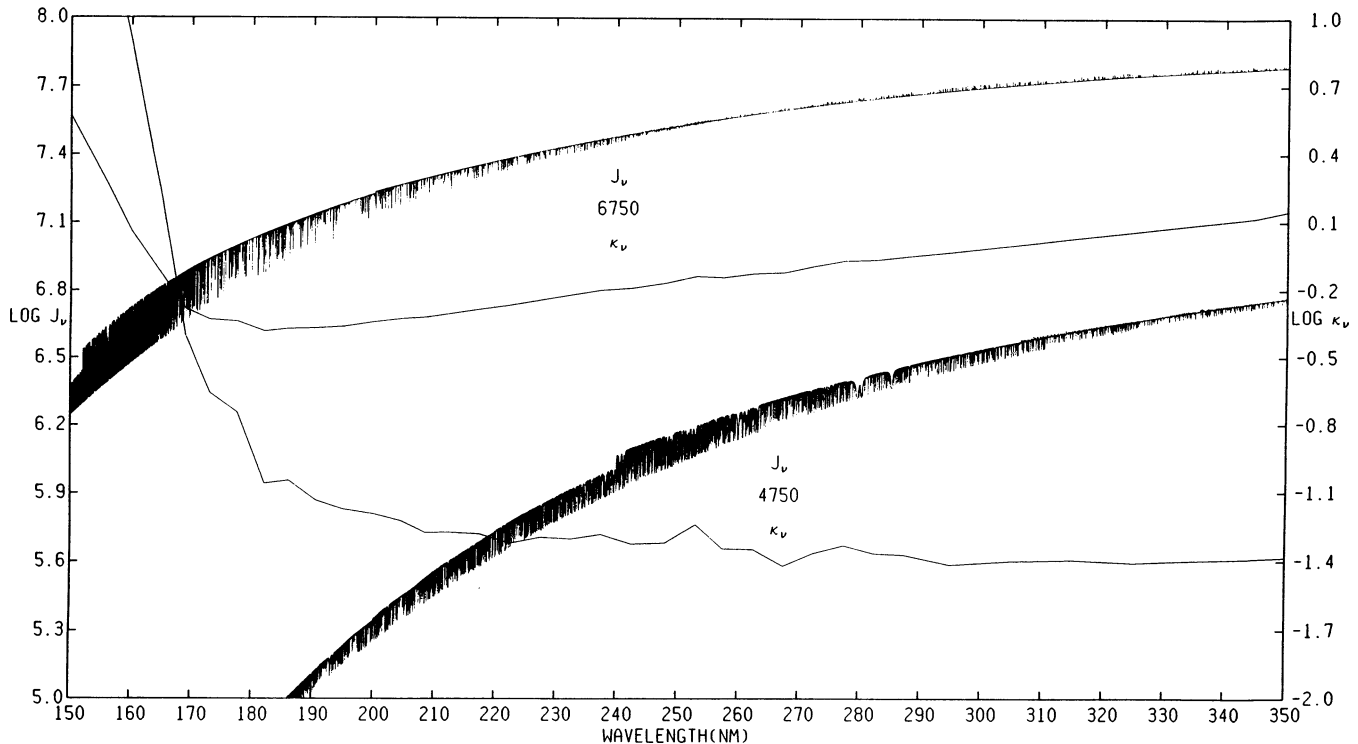


FIG. 7.—The mean intensity  $J_\nu$  in  $\text{ergs cm}^{-2} \text{s}^{-1} \text{sr}^{-1}$  and total opacity  $\kappa_\nu$  in  $\text{cm}^2 \text{g}^{-1}$  in the Balmer continuum for the hot and cold models at the depth of formation of the D lines in the mean model. The  $\text{Li } ^2S$  continuum starts at 230 nm. The  $\text{Li } ^2P$  continuum starts at 350 nm. The mean intensity is between 1–2 orders of magnitude greater in the hot component. The cold component is about 15 times more transparent.

It is easy for the reader to check these calculations or to extend them to other temperature and abundance ranges. The model atmosphere program ATLAS9 and 6000 model atmospheres, including the ones used here, are given on Kurucz CD-ROM 13 (1993b). The spectrum synthesis program that was used to compute the LTE line profiles is on Kurucz CD-ROM 18 (1993c). All the line data for the lithium D region are given in Tables 1 and 2. Non-LTE was insignificant to the calculations in this paper. For other temperatures and gravities, non-LTE corrections can be estimated from the tables of Carlsson et al. (1994).

Elements other than Li may be affected as well. At the same depth as for Li, Ca is 99.9% ionized; Na is 99.5% ionized, and Fe is 97.8% ionized. The metallicity may be determined incorrectly. Be and B may be safe, 78.5% and 69.8%. The hydrides and CO are probably very sensitive.

Problems like this can arise in any convective atmosphere for any species that does not average in space and time to the one-dimensional model predictions. In the Sun this may account for the remaining uncertainties with Fe I found by Blackwell, Lynas-Gray, & Smith (1995) and for the cool CO fundamental line cores (Ayres & Testerman 1981). Problems with K giant abundances may also arise from similar mechanisms. Because of the hot and cold components, the ultraviolet photospheric flux in any convective star must be higher than a one-dimensional model predicts (Bikmaev 1994). Then, by flux conservation, the flux redward of the flux maximum must be lower. It is fitted by a model with lower effective temperature than that of the star. This flux "distortion" may be responsible for Short & Lester's (1994) problems with the ultraviolet flux of Arcturus.

The following qualitative predictions result from the exponential falloff of the flux blueward of the flux maximum:

1. The Balmer continuum in all convective stars is higher than predicted by a one-dimensional model.
2. In G stars, including the Sun, the discrepancy reaches up to about 400 nm.
3. In K stars the discrepancy reaches to about 500 nm.

4. In M stars the whole Paschen continuum is higher.

5. Flux from a temperature minimum and a chromospheric temperature rise masks this photospheric effect at short wavelengths, but the increased mean intensity still affects photoionization rates in photospheric non-LTE calculations.

6. The spectrum predicted from a one-dimensional model for the exponential falloff region, and abundances derived therefrom, are systematically in error.

7. Limb darkening predicted from a one-dimensional model for the exponential falloff region is systematically in error.

## 6. CONCLUSIONS

The D lines of Li I in extreme Population II stars hotter than 5500 K are highly temperature sensitive because lithium is nearly all ionized. A one-dimensional model atmosphere represents a space and time average over the real three-dimensional moving hot and cold convective structure. Neutral Li does not have the average behavior represented by the one-dimensional model. Lithium is overionized by a factor of 10 so that the Li abundance computed from a one-dimensional model is too small by this same factor. Consequently,  $\log(N_{\text{Li}}/N_{\text{total}}) + 12 > 3.0$ .

Convective model atmospheres must be used with caution when the properties predicted by the model, such as those listed above, may not represent the space and time average of the real properties of stars.

This higher Li abundance resolves the only discrepancy in the radiatively driven cosmological model of the universe discussed by Kurucz (1993a). Because the baryon density is high enough to produce a flat, or nearly flat, universe, the number of stars can increase by a factor of 10, and the amount of radiation given off by those stars in the first billion years can increase by a factor of 10 over what is possible with a low baryon density.

I thank Eugene Avrett for his critical editing. This work was supported in part by NASA grants NAGW-1486, NAGW-2528, and NAGW-3299.

## REFERENCES

- Ayres, T. R., & Testerman, L. 1981, *ApJ*, 245, 1124  
 Bikmaev, I. 1994, private communication  
 Blackwell, D. E., Lynas-Gray, A. E., & Smith, G. 1995, *A&A*, 296, 217  
 Boesgaard, A. M., & Steigman, G. 1985, *ARA&A*, 23, 319  
 Carlsson, M., Rutten, R. J., Bruls, J. H. M. J., & Shchukina, N. G. 1994, *A&A*, 288, 860  
 Chan, K. L., Nordlund, Å., Steffen, M., & Stein, R. F. 1991, *Solar Interior and Atmosphere* (Tucson: Univ. Arizona Press)  
 Corliss, C. H., & Bozman, W. R. 1962, *Experimental Transition Probabilities for Spectral Lines of Seventy Atoms* (NBS Monograph 53)  
 Corliss, C. H., & Warner, B. 1964, *ApJS*, 8, 395  
 D'Antona, F., & Mazzitelli, I. 1984, *A&A*, 138, 431  
 Goldberg, L., Kopp, R. A., & Dupree, A. K. 1964, *ApJ*, 140, 707  
 Goldberg, L., Müller, E., & Aller, L. H. 1960, *ApJS*, 8, 395  
 Hobbs, L. M., & Thorburn, J. 1994, *ApJ*, 428, L25  
 Kolb, E. W., & Turner, M. S. 1990, *The Early Universe* (Reading, MA: Addison-Wesley)  
 Kurucz, R. L. 1992, *Comments Astrophys.*, 16, 1  
 ———. 1993a, *Radiatively Driven Cosmology*, unpublished  
 Kurucz, R. L. 1993b, *ATLAS9 Stellar Atmosphere Programs and 2 km s grid* (Kurucz CD-ROM No. 13)  
 ———. 1993c, *SYNTH3 Spectrum Synthesis Programs and Line Data* (Kurucz CD-ROM No. 18)  
 Kurucz, R. L., Furenlid, I., Brault, J., & Testerman, L. 1984, *Solar Flux Atlas from 296 to 1300 nm* (Sunspot, NM: National Solar Observatory)  
 Lubowich, D. A., Pasachoff, J. M., Galloway, R. P., Kurucz, R. L., & Smith, V. V. 1994, *BAAS*, 26, 1479  
 Michaud, G., Fontaine, G., & Beaudet, G. 1984, *ApJ*, 282, 206  
 Molaro, P., Bonifacio, P., & Primas, F. 1995, *Mem. Soc. Astron. Italiana*, in press  
 Nave, G., Johansson, S., Learner, R. C. M., Thorne, A. P., & Brault, J. W. 1994, *ApJS*, 94, 221  
 Nordlund, Å., & Dravins, D. 1990, *A&A*, 228, 155  
 Rebolo, R., Molaro, P., & Beckman, J. 1988, *A&A*, 192, 192  
 Short, C. I., & Lester, J. B. 1994, *ApJ*, 436, L365  
 Spite, F., & Spite, M. 1982, *A&A*, 163, 140  
 Topka, K. P., & Title, A. M. 1991, *Solar Interior and Atmosphere* (Tucson: Univ. Arizona Press)